

Solid-State and Solution Structure of a Hypervalent AX_5 Compound: $\text{Sb}(\text{C}_6\text{F}_5)_5^{**}$

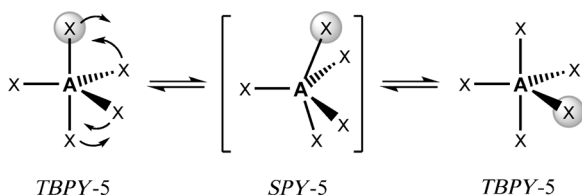
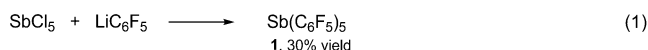
M. Angeles García-Monforte, Pablo J. Alonso, Irene Ara, Babil Menjón,* and Pilar Romero

Dedicated to Professor Gerhard Erker on the occasion of his 65th birthday

“There is no more basic enterprise in chemistry than the determination of the geometrical structure of a molecule”.^[1] Detailed knowledge of the molecular structure of a chemical species in the solid state—usually established by X-ray and/or neutron diffraction techniques—should be complemented, wherever possible, with information on its structure in solution.^[2] The fulfilment of this two-fold task is particularly difficult in the case of pentasubstituted compounds, since they are especially prone to undergo intramolecular stereomutation processes in solution.^[3] This fluxional behavior is mainly due to the low energy separation between the most common geometries: trigonal bipyramidal (*TBPY*-5) and square pyramidal (*SPY*-5, Scheme 1).^[4] Paradigmatic examples of this

estimate the energy barrier ($E_a = 7(1) \text{ kJ mol}^{-1}$) associated to the CO-scrambling process in liquid $\text{Fe}(\text{CO})_5$ by careful analysis of ultrafast two-dimensional IR spectroscopic results.^[7] Here we report on the molecular structure of a hypervalent^[8] AX_5 compound, $\text{Sb}(\text{C}_6\text{F}_5)_5$, both in the solid state and in solution together with a detailed analysis of its fluxional behavior in solution.

$\text{Sb}(\text{C}_6\text{F}_5)_5$ (**1**) has been obtained in reasonable yield by low-temperature treatment of SbCl_5 with LiC_6F_5 in $\text{Et}_2\text{O}/n$ -hexane [Eq. (1)]. Compound **1** is an air-stable, white solid



Scheme 1. Berry pseudorotation mechanism by which identical substituents located in axial (ax) and equatorial (eq) positions of a trigonal bipyramid (*TBPY*-5) exchange their positions through a square pyramidal (*SPY*-5) transition state.

behavior are the well-known PF_5 and $\text{Fe}(\text{CO})_5$ molecules, the NMR spectra of which show in solution a single signal for all five substituents (^{19}F ^[5] or ^{13}CO ^[6] respectively) even at the lowest temperatures attainable. The activation energy associated with the stereomutation process operating in these model species is so low that it is very difficult to determine experimentally. In fact, it has only recently been possible to

that sublimates at 95°C and 10^{-1} Torr. At this point it is appropriate to comment on a report that has recently appeared in patent literature claiming the synthesis of **1** by reaction of SbCl_5 with $\text{Zn}(\text{C}_6\text{F}_5)_2$.^[9] Very few synthetic details and no physical, analytic, or spectroscopic properties of the final product are given therein. However, it is stated that “unreacted bis(pentafluorophenyl)zinc may be removed through sublimation at a pressure of 10^{-2} Torr and 110°C .” This statement alone would raise doubts about the result, since compound **1** also sublimates under the given conditions and thus, if really formed, would be lost together with $\text{Zn}(\text{C}_6\text{F}_5)_2$ in the sublimate.

Compound **1** belongs to the class of neutral, homoleptic organopnictogen(V) derivatives, ER_5 ($\text{E} = \text{P}, \text{As}, \text{Sb}, \text{Bi}$). The solid-state molecular structures of the whole phenyl series ($\text{R} = \text{Ph}$) are known and the observed group trend is especially intriguing. *TBPY*-5 structures were found for the phenyl-derivatives of the lighter elements P ^[10] and As ,^[11] in keeping with the VSEPR model.^[12] In contrast, a *SPY*-5 geometry was found for the 6th period element Bi .^[13] Antimony occupies the inflection point in the series, since *SPY*-5 and *TBPY*-5 structures were respectively established for SbPh_5 ^[14] and the solvate $\text{SbPh}_5 \cdot 0.5 \text{ CyH}$.^[15] The fact that simple lattice effects are able to decide between the two SbPh_5 polytopes, suggests a small energy difference between them. This observation is in keeping with the highly fluxional behavior of all these ER_5 molecules in solution.^[16]

The crystal and molecular structures of **1** were established by single-crystal X-ray diffraction methods. The local environment of the Sb center (Figure 1) can be described as *TBPY*-5 according to the low continuous shape measure (CSHM) value^[17] obtained for that geometry: $S(\text{TBPY}-5) = 0.40$.^[18] The axial positions are virtually in line with the central

[*] Dr. M. A. García-Monforte, Dr. I. Ara, Dr. B. Menjón
Instituto de Síntesis Química y Catálisis Homogénea (ISQCH)
Universidad de Zaragoza-C.S.I.C.
C/Pedro Cerbuna 12, 50009 Zaragoza (Spain)
E-mail: menjon@unizar.es

Prof. Dr. P. J. Alonso, Dr. P. Romero
Instituto de Ciencia de Materiales de Aragón (ICMA)
Universidad de Zaragoza-C.S.I.C.
C/Pedro Cerbuna 12, 50009 Zaragoza (Spain)

[**] This work was supported by the Spanish MICINN (DGPTC)/FEDER (project number CTQ2008-06669-C02-01/BQU) and the Gobierno de Aragón (Grupo Consolidado E21: Química Inorgánica y de los Compuestos Organometálicos).

Supporting information for this article is available on the WWW under <http://dx.doi.org/10.1002/anie.201108858>.

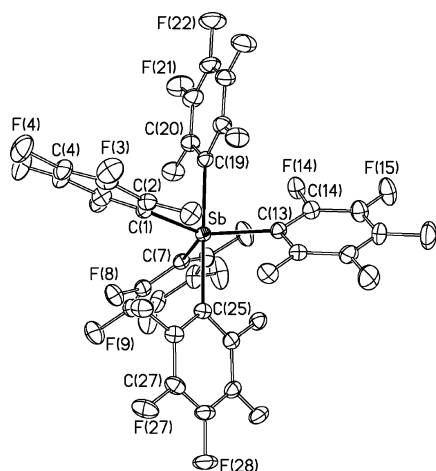


Figure 1. Thermal ellipsoid diagram (50% probability) of $\text{Sb}(\text{C}_6\text{F}_5)_5$ as found in single crystals of $1.0.25 \text{ C}_6\text{H}_{14}$. Selected bond lengths [pm] and angles [°] with estimated standard deviations: average $\text{Sb}-\text{C}_{\text{eq}}$ 214.7(3), average $\text{Sb}-\text{C}_{\text{ax}}$ 222.7(3), $\text{C}(1)-\text{Sb}-\text{C}(7)$ 113.9(1), $\text{C}(1)-\text{Sb}-\text{C}(13)$ 124.5(1), $\text{C}(7)-\text{Sb}-\text{C}(13)$ 121.6(1), $\text{C}(19)-\text{Sb}-\text{C}(25)$ 178.8(1).

atom, but a slight *Y* distortion is observed in the equatorial plane. The axial $\text{Sb}-\text{C}$ bonds are significantly longer than the equatorial ones (222.7(3) vs. 214.7(3) pm average values), probably as the result of a 3-center/4-electron hypervalent bond in the axial direction.^[8] The difference between axial and equatorial $\text{E}-\text{C}$ bond lengths is less pronounced in the related open-shell, paramagnetic organotransition-metal derivatives $[\text{M}^{\text{III}}(\text{C}_6\text{F}_5)_5]^{2-}$ ($\text{M}^{\text{III}} = \text{Ti}^{\text{III}}$ (d^1),^[19] V^{III} (d^2)^[20]), which also show roughly similar *TBPY*-5 geometries.

The ^{19}F NMR spectrum of **1** in CD_2Cl_2 solution at room temperature (313 K) displays a single set of signals, one for each kind of *ortho*-, *meta*-, and *para*-F substituents (Figure 2). At low temperature (183 K), however, each signal splits into pairs with 3:2 relative integrated ratio (Figure 2). This spectroscopic behavior allows us to conclude that compound **1** has a *TBPY*-5 geometry also in solution and that it readily undergoes stereomutation. The activation energy, E_a , associated with this dynamic process was determined by line-shape analysis of the thermal dependence of the ^{19}F NMR spectrum of **1** between the slow and the rapid exchange limits (Figure 3). A common value of $E_a = 24.4(4) \text{ kJ mol}^{-1}$ was obtained from the analysis of all three nonindependent sets of signals corresponding to the *ortho*-, *meta*-, and *para*-F substituents (see the Supporting Information for details). The result obtained can thus be considered to be highly reliable.

As far as we know, all previous attempts to detect the limiting slow-exchange spectrum in homoleptic organopnictogen(V) derivatives, ER_5 , have failed.^[16] Efforts to widen the frequency range of the observed nucleus by introducing fluorinated substituents as in $\text{Sb}[\text{C}_6\text{H}_4(\text{CF}_3)-4]_5$ did not yield any improvement.^[16a] No better results were attained when the methyl group in SbMe_5 was replaced by the sterically demanding CH_2SiMe_3 , as $\text{Sb}(\text{CH}_2\text{SiMe}_3)_5$ also gave a single type of ligand down to 153 K.^[21] In contrast,

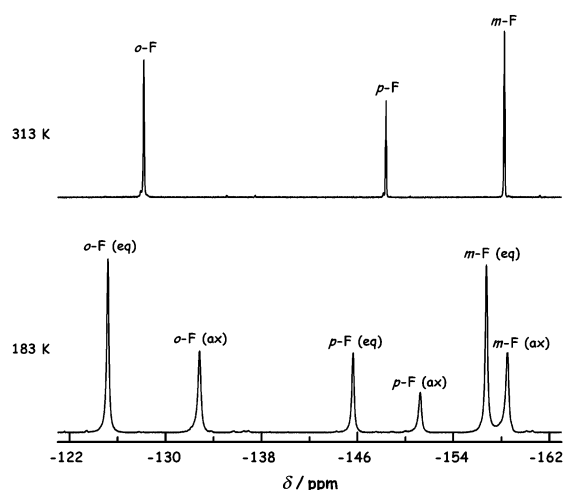


Figure 2. ^{19}F NMR spectra of **1** in CD_2Cl_2 solution evidencing rapid (313 K) and slow (183 K) limiting exchange conditions. The 3:2 integrated ratio for each kind of F substituent in the later spectrum evidences a *TBPY*-5 structure in the slow exchange limit.

replacement of just one of the C_6F_5 substituents in **1** by the less sterically demanding *n*-butyl group resulted in the heteroleptic species $\text{Sb}(\text{C}_6\text{F}_5)_4^{\text{n}}\text{Bu}$ (**2**), which is highly fluxional in CD_2Cl_2 solution even at 183 K. The solid-state structure of **2** (Figure 4) also approaches a *TBPY*-5 geometry with a CShM value^[17] of $S(\text{TBPY}-5) = 0.46$.^[18] The less electronegative *n*-butyl group is located in an equatorial position, as is usually found in pentasubstituted hypervalent compounds with *TBPY*-5 geometry.^[22] As in SbPh_3Me_2 ,^[23] there is no difference between the $\text{Sb}-\text{C}(\text{alkyl})$ and $\text{Sb}-\text{C}(\text{aryl})$ bond lengths, but there is a difference between the $\text{Sb}-\text{C}(\text{ax})$ and $\text{Sb}-\text{C}(\text{eq})$ ones. The average $\text{Sb}-\text{C}(\text{ax})$ bond

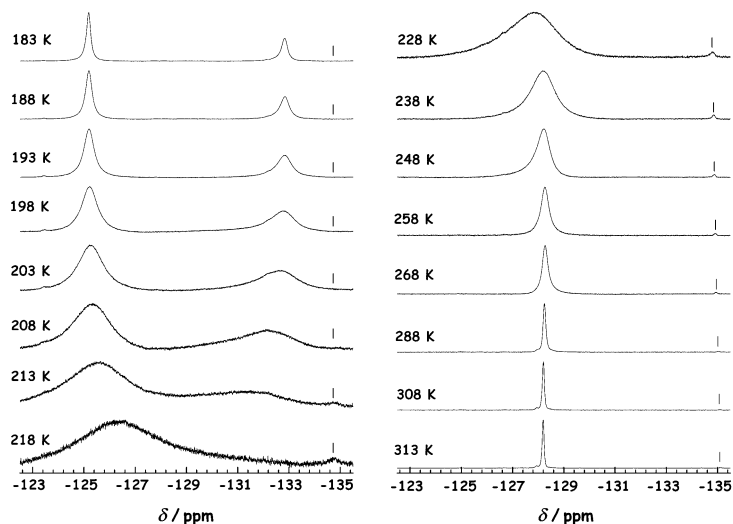


Figure 3. ^{19}F NMR spectrum of **1** in CD_2Cl_2 solution at variable temperature showing the thermal evolution of the *ortho*-F signals. Vertical scale adjustment has been applied to each individual spectrum. The marked signal corresponds to a tiny impurity not involved in the fluxional process. For the thermal evolution of the *meta*-F and the *para*-F signals together with a line-shape analysis of all of these spectra see the Supporting Information.

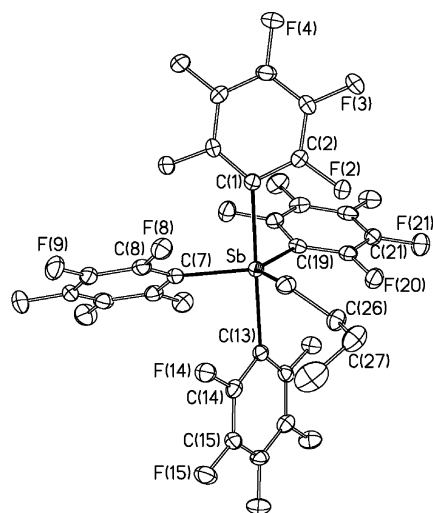


Figure 4. Thermal ellipsoid diagram (50% probability) of **2**. Selected bond lengths [pm] and angles [°] with estimated standard deviations: Sb–C(1) 227.7(2), Sb–C(7) 212.3(2), Sb–C(13) 227.4(2), Sb–C(19) 213.7(2), Sb–C(25) 214.3(2), C(1)–Sb–C(13) 175.4(1), C(7)–Sb–C(19) 118.0(1), C(7)–Sb–C(25) 114.5(1), C(19)–Sb–C(25) 127.4(1).

length in **2** (227.5(2) pm) is slightly longer than in **1** (222.7(3) pm), whereas the opposite applies for the average Sb–C(eq) value: 213.4(2) pm in **2** vs. 214.7(3) in **1**. There is no obvious reason for the rather different C(alkyl)–Sb–C(aryl) angles formed between the *n*Bu group and the equatorial C₆F₅ ones: 114.48(9)° vs. 127.45(9)°. Nevertheless, the sum of all equatorial C–Sb–C' angles virtually amounts to 360°.

To summarize, in contrast to the structural dichotomy shown by Sb(C₆H₅)₅ in the solid state depending on the crystal environment,^[14,15] the perfluorinated derivative Sb(C₆F₅)₅ (**1**) has been found to favor the *TBPY*-5 geometry both in the solid state and in solution. Even so, compound **1** is also stereochemically nonrigid in solution. The activation energy of the operating stereomutation process has been experimentally determined. The value obtained, $E_a = 24.4(4)$ kJ mol^{−1}, sets the upper limit for the energy separation between the *TBPY*-5 (lower-energy state) and *SPY*-5 (transition state) geometries.

Experimental Section

General working techniques are described in ref. [24]. Additionally, a Bruker AV 500 spectrometer was used to obtain the variable-temperature ¹⁹F NMR spectroscopic data.

1: A freshly prepared solution of SbCl₅ (1.18 g, 3.94 mmol) in *n*-hexane (15 cm³) was added dropwise to a solution of LiC₆F₅ (13.81 mmol) in Et₂O (60 cm³) at −78°C. A white precipitate formed while the temperature of the mixture was allowed to slowly reach 0°C. After 15 h of stirring at that temperature, the white solid in suspension was separated by filtration and further extracted in CH₂Cl₂ (30 cm³). The extract was concentrated to dryness and the resulting residue was treated with *n*-hexane (5 cm³). A white solid was eventually obtained, which was filtered, washed with *n*-hexane (3 × 2 cm³), and vacuum dried (**1**: 1.1 g, 1.15 mmol, 30% yield). Satisfactory elemental analysis. IR (KBr): $\tilde{\nu}_{\max} = 1637$ (m), 1516 (s), 1487 (s), 1465 (s), 1379 (m), 1360 (m), 1284 (w), 1274 (w), 1148 (w), 1086 (s), 1074 (s), 1001 (w), 976 (s; C–F), 965 (s; C–F), 793 (w; C₆F₅: X-sensitive),^[25] 750 (w), 721 (w), 623 (w), 584 (w), 484 (w), 380 cm^{−1} (w).

¹⁹F NMR (470.385 MHz, CD₂Cl₂, 313 K): $\delta = -128.2$ (2F, *o*-F), −148.4 (1F, *p*-F), −158.2 ppm (2F, *m*-F). ¹⁹F NMR (470.385 MHz, CD₂Cl₂, 183 K): $\delta = -125.2$ (6F, *o*-F(eq)), −132.8 (4F, *o*-F(ax)), −145.6 (3F, *p*-F(eq)), −151.2 (2F, *p*-F(ax)), −156.7 (6F, *m*-F(eq)), −158.5 ppm (4F, *m*-F(ax)). MS (MALDI+, DCTB) $m/z = 937$ [Sb(C₆F₅)₄(C₆F₄)₄]⁺, 789 [Sb(C₆F₅)₄]⁺.

Crystal data for **1**: 0.25 C₆H₁₄: Single crystals suitable for X-ray diffraction purposes were obtained by slow evaporation at 4°C of a CHCl₃–*n*-hexane solution of **1**. C_{31.5}H_{3.5}F₂₅Sb; triclinic; space group *P* $\bar{1}$; $a = 1104.20(5)$, $b = 1133.00(5)$, $c = 1417.28(6)$ pm, $\alpha = 76.135(1)$, $\beta = 69.095(1)$, $\gamma = 84.210(1)^\circ$, $V = 16.0789(12)$ nm³; $Z = 2$; $T = 100(2)$ K; $\lambda = 71.073$ pm; absorption coefficient 1.029 mm^{−1}, range for data collection $1.97 < \theta < 28.75^\circ$; reflections collected/unique: 15303/7549 ($R_{\text{int}} = 0.0206$); Bruker Smart CCD diffractometer. The crystallographic data were corrected for absorption with SADABS.^[26] The structure was solved by direct methods and refinement against F^2 with SHELXL-97^[27] converged to final residual indices of $R_1 = 0.0341$, $wR_2 = 0.0868$ [$I > 2\sigma(I)$] and $R_1 = 0.0388$, $wR_2 = 0.0890$ (all data). GoF = 1.034.

2: A freshly prepared solution of SbCl₅ (1.18 g, 3.94 mmol) in *n*-hexane (20 cm³) was added dropwise to a *n*-hexane (30 cm³) solution containing LiC₆F₅ (19.7 mmol) and Li^{*i*}Bu (3.9 mmol) at −78°C. The mixture was allowed to slowly reach room temperature and, after a further 20 h of stirring, it was filtered. The filtrate was concentrated to dryness yielding an oil which was extracted in Et₂O (5 cm³). The extract was cooled to −50°C and *n*-hexane (15 cm³) was added dropwise under vigorous stirring until a white solid separated. The solid was filtered, washed at 0°C with *i*PrOH, (3 × 1 cm³) and vacuum dried. By allowing the mother liquor to stand at −30°C for 3 days, a second crop was obtained (**2**: 0.5 g, 0.6 mmol, 15% joint yield). Satisfactory elemental analysis. IR (KBr): $\tilde{\nu}_{\max} = 2968$ (w), 2881 (w), 1640 (m), 1513 (s), 1489 (s), 1484 (s), 1458 (s), 1438 (m), 1385 (m), 1347 (m), 1281 (w), 1266 (m), 1183 (w), 1142 (w), 1085 (s), 1071 (s), 1015 (w), 972 (s; C–F), 959 (s; C–F), 895 (w), 799 (w; C₆F₅: X-sensitive),^[25] 748 (w), 720 (w), 705 (w), 622 (w), 608 (w), 582 (w), 480 (w), 388 (w), 369 (w), 361 cm^{−1} (w). ¹H NMR (400 MHz, CD₂Cl₂, 298 K): $\delta = 3.23$ (tt, 2H, α -H, $^3J(\text{H}^\alpha, \text{H}^\beta) = 7.8$ Hz, $^4J(\text{H}^\alpha, \text{H}^\gamma) \approx 0.4$ Hz), 1.79 (m, 2H, β -H, $^3J(\text{H}^\beta, \text{H}^\gamma) = 7.5$ Hz, $^4J(\text{H}^\beta, \text{H}^\delta) \approx 0.4$ Hz), 1.44 (m, 2H, γ -H, $^3J(\text{H}^\gamma, \text{H}^\delta) = 7.5$ Hz), 0.90 ppm (tt, 3H, δ -H). ¹⁹F NMR (282.231 MHz, CD₂Cl₂, 298 K): $\delta = -130.4$ (2F, *o*-F), −152.6 (1F, *p*-F), −161.2 ppm (2F, *m*-F). MS (MALDI+, DCTB) $m/z = 789$ [Sb(C₆F₅)₄]⁺, 679 [Sb(C₆F₅)₃(C₆H₉)]⁺, 569 [Sb(C₆F₅)₂F₃(C₆H₉)]⁺.

Crystal data for **2**: Single crystals suitable for X-ray diffraction purposes were obtained by slow diffusion of a *n*-hexane layer into a Et₂O solution of **2** at −30°C. C₂₈H₆F₂₀Sb; monoclinic; space group *P*₂₁/*n*; $a = 1143.87(6)$, $b = 1344.51(7)$, $c = 1791.02(9)$ pm, $\beta = 94.202(1)^\circ$, $V = 27.471(2)$ nm³; $Z = 4$; $T = 100(2)$ K; $\lambda = 71.073$ pm; absorption coefficient 1.162 mm^{−1}, range for data collection $1.90 < \theta < 28.81^\circ$; reflections collected/unique: 24647/6658 ($R_{\text{int}} = 0.0311$); Bruker Smart CCD diffractometer. The crystallographic data were corrected for absorption with SADABS.^[26] The structure was solved by direct methods and refinement against F^2 with SHELXL-97^[27] converged to final residual indices of $R_1 = 0.0296$, $wR_2 = 0.0649$ [$I > 2\sigma(I)$] and $R_1 = 0.0371$, $wR_2 = 0.0675$ (all data). GoF = 1.003.

CCDC 856956 (**1**; 0.25 C₆H₁₄) and 856957 (**2**) contain the supplementary crystallographic data for this paper. These data can be obtained free of charge from The Cambridge Crystallographic Data Centre via www.ccdc.cam.ac.uk/data_request/cif.

Received: December 15, 2011

Revised: January 18, 2012

Published online: February 3, 2012

Keywords: hypervalent compounds · organometallic chemistry · structure elucidation

- [1] R. Hoffmann, *Am. Sci.* **1998**, 86, 15.
- [2] E. L. Muetterties, *Inorg. Chem.* **1965**, 4, 769.
- [3] C. Moberg, *Angew. Chem.* **2011**, 123, 10473; *Angew. Chem. Int. Ed.* **2011**, 50, 10290; E. P. A. Couzijn, J. C. Slootweg, A. W. Ehlers, K. Lammertsma, *J. Am. Chem. Soc.* **2010**, 132, 18127; K. Seppelt, *Chem. Unserer Zeit* **1975**, 9, 10; F. A. Cotton, *J. Organomet. Chem.* **1975**, 100, 29; *Dynamic Nuclear Magnetic Resonance Spectroscopy* (Eds.: L. M. Jackman, F. A. Cotton), Academic Press, New York, **1975**; E. L. Muetterties, *Acc. Chem. Res.* **1970**, 3, 266; R. S. Berry, *J. Chem. Phys.* **1960**, 32, 933.
- [4] R. R. Holmes, *Prog. Inorg. Chem.* **1984**, 32, 119; D. Hellwinkel, *Top. Curr. Chem.* **1983**, 109, 1; H. Schmidbaur, *Adv. Organomet. Chem.* **1976**, 14, 205; J. S. Wood, *Prog. Inorg. Chem.* **1972**, 16, 227; R. R. Holmes, *Acc. Chem. Res.* **1972**, 5, 296; E. L. Muetterties, R. A. Schunn, *Q. Rev. Chem. Soc.* **1966**, 20, 245.
- [5] H. S. Gutowsky, D. W. McCall, C. P. Slichter, *J. Chem. Phys.* **1953**, 21, 279.
- [6] R. Bramley, B. N. Figgis, R. S. Nyholm, *Trans. Faraday Soc.* **1962**, 58, 1893; F. A. Cotton, A. Danti, J. S. Waugh, R. W. Fessenden, *J. Chem. Phys.* **1958**, 29, 1427.
- [7] J. F. Cahoon, K. R. Sawyer, J. P. Schlegel, C. B. Harris, *Science* **2008**, 319, 1820.
- [8] G. S. McGrady, J. W. Steed in *Encyclopedia of Inorganic Chemistry*, Vol. 3 (Ed.: R. B. King), Wiley, Chichester, **2005**, pp. 1938–1959; *Chemistry of Hypervalent Compounds* (Ed.: K.-y. Akiba), Wiley-VCH, Weinheim, **1999**.
- [9] S. P. Lewis, US Patent No. 7585991, **2009** [*Chem. Abstr.* **2008**, 149, 176788].
- [10] G. Müller, U. J. Bildmann, *Z. Naturforsch. B* **2004**, 59, 1411; P. J. Wheatley, *J. Chem. Soc.* **1964**, 2206.
- [11] C. P. Brock, D. F. Webster, *Acta Crystallogr. Sect. B* **1976**, 32, 2089.
- [12] R. J. Gillespie, P. L. A. Popelier, *Chemical Bonding and Molecular Geometry*, Oxford University Press, New York, **2001**, chap. 4, pp. 84–112; R. J. Gillespie, I. Hargittai, *The VSEPR Model of Molecular Geometry*, Allyn and Bacon, Boston, MA, **1991**, pp. 55–57.
- [13] A. Schmuck, J. Buschmann, J. Fuchs, K. Seppelt, *Angew. Chem.* **1987**, 99, 1206; *Angew. Chem. Int. Ed. Engl.* **1987**, 26, 1180.
- [14] A. L. Beauchamp, M. J. Bennett, F. A. Cotton, *J. Am. Chem. Soc.* **1968**, 90, 6675; P. J. Wheatley, *J. Chem. Soc.* **1964**, 3718; P. J. Wheatley, G. Wittig, *Proc. Chem. Soc.* **1962**, 251.
- [15] C. Brabant, B. Blanck, A. L. Beauchamp, *J. Organomet. Chem.* **1974**, 82, 231.
- [16] a) G. Schröder, T. Okinaka, Y. Mimura, M. Watanabe, T. Matsuzaki, A. Hasuoka, Y. Yamamoto, S. Matsukawa, K.-y. Akiba, *Chem. Eur. J.* **2007**, 13, 2517; b) G. L. Kuykendall, J. L. Mills, *J. Organomet. Chem.* **1976**, 118, 123; c) I. R. Beattie, K. M. S. Livingston, G. A. Ozin, R. Sabine, *J. Chem. Soc. Dalton Trans.* **1972**, 784.
- [17] The continuous shape measure (CShM), *S*, is one of the most plausible attempts to accurately describe real molecules in terms of geometric polyhedra. Following its mathematical definition, deviations from a given polyhedron in bond lengths as well as in interbond angles both contribute to increase the *S* value. Thus, the smaller the value of *S*, the better the agreement between the real molecule and the suggested model, *S*=0 for perfect coincidence: M. Pinsky, D. Avnir, *Inorg. Chem.* **1998**, 37, 5575. M. Llunell, D. Casanova, J. Cirera, J. M. Bofill, P. Alemany, S. Alvarez, M. Pinsky, D. Avnir, *SHAPE*, Version 1.1b 02t, Universitat de Barcelona and The Hebrew University of Jerusalem.
- [18] S. Alvarez, M. Llunell, *J. Chem. Soc. Dalton Trans.* **2000**, 3288.
- [19] P. J. Alonso, L. R. Falvello, J. Forniés, M. A. García-Monforte, B. Menjón, *Angew. Chem.* **2004**, 116, 5337; *Angew. Chem. Int. Ed.* **2004**, 43, 5225.
- [20] P. J. Alonso, J. Forniés, M. A. García-Monforte, A. Martín, B. Menjón, *Chem. Eur. J.* **2005**, 11, 4713.
- [21] H. Schmidbaur, G. Haßlberger, *Chem. Ber.* **1978**, 111, 2702.
- [22] R. Hoffmann, J. M. Howell, E. L. Muetterties, *J. Am. Chem. Soc.* **1972**, 94, 3047; E. L. Muetterties, W. Mahler, K. J. Packer, R. Schmutzler, *Inorg. Chem.* **1964**, 3, 1298; E. L. Muetterties, W. Mahler, R. Schmutzler, *Inorg. Chem.* **1963**, 2, 613.
- [23] S. Wallenhauer, K. Seppelt, *Inorg. Chem.* **1995**, 34, 116.
- [24] S. Martínez-Salvador, J. Forniés, A. Martín, B. Menjón, *Chem. Eur. J.* **2011**, 17, 8085.
- [25] R. Usón, J. Forniés, *Adv. Organomet. Chem.* **1988**, 28, 219; E. Maslowsky, Jr., *Vibrational Spectra of Organometallic Compounds*, Wiley, New York, **1977**, pp. 437–442.
- [26] G. M. Sheldrick, *SADABS: Program for area detector absorption correction*, Version 2.03, University of Göttingen, Göttingen (Germany), **1996**.
- [27] G. M. Sheldrick, *SHELXL-97: Program for the refinement of crystal structures from diffraction data*, University of Göttingen, Göttingen (Germany), **1997**.